Modeling and assessing the influence of linear energy transfer on multiple bit upset susceptibility*

Geng Chao(耿 超)[a)b)], Liu Jie(刘 杰)[a)†], Xi Kai(习 凯)[a)b)],
Zhang Zhan-Gang(张战刚)[a)b)], Gu Song(古 松)[a)b)], and Liu Tian-Qi(刘天奇)[a)b)]

[a)] *Institute of Modern Physics, Chinese Academy of Sciences, Lanzhou* 730000, *China*
[b)] *University of Chinese Academy of Sciences, Beijing* 100190, *China*

(Received 29 January 2013; revised manuscript received 6 March 2013)

The influence of the metric of linear energy transfer (LET) on single event upset (SEU), particularly multiple bit upset (MBU) in a hypothetical 90-nm static random access memory (SRAM) is explored. To explain the odd point of higher LET incident ion but induced lower cross section in the curve of SEU cross section, MBUs induced by incident ions ^{132}Xe and ^{209}Bi with the same LET but different energies at oblique incidence are investigated using multi-functional package for single event effect analysis (MUFPSA). In addition, a comprehensive analytical model of the radial track structure is incorporated into MUFPSA, which is a complementation for assessing and interpreting MBU susceptibility of SRAM. The results show that (i) with the increase of incident angle, MBU multiplicity and probability each present an increasing trend; (ii) due to the higher ion relative velocity and longer range of δ electrons, higher energy ions trigger the MBU with less probability than lower energy ions.

Keywords: MUFPSA, LET, MBU, ion track structure

PACS: 95.75.–z, 61.82.Fk, 24.10.Lx **DOI:** 10.1088/1674-1056/22/10/109501

1. Introduction

The device susceptibility to single event effect (SEE),[1–5] induced by high energetic particles in radiation environment, is often vital to its applicability and reliability in submicrometer electronic technologies. Notably, the devices with reducing size, nanoscale in particular, have become increasingly sensitive to single event upset (SEU)[6–11] and multiple bit upset (MBU)[12–17] effects. Meanwhile, the highly developed integrated circuits have been performing a reducing critical charge that is necessary to trigger the SEE.

Both the radiation environment, to which the devices are exposed, and the intrinsic properties of the device (e.g. data pattern, varying voltage) have a significant effect on SEE sensitivity in submicron devices. Radiation features (e.g. ion species, ion energy) as significant essentials in the radiation environment fulfill an important function in device testing. Many previous studies have been carried out to elucidate the SEE as a function of the radiation feature in terms of linear energy transfer (LET).[1–5] However, LET has not been accepted as the exclusive engineering metric to analyze and characterize SEEs. For instance, Stapor *et al.*[7] demonstrated that the higher energy ions caused more charges to be collected due to less initial e^-/h^+ pair recombination and more diffusion of higher energy track, even though all incident ions have the same LET. Later, Dodd *et al.*[8] analyzed the effects of heavy ion energy in CMOS SRAMs, which turned out significant differences in SEU cross section between low- and high-energy heavy ions radiation. Similarly, the limitations and inaccuracies of LET have been interpreted in Refs. [9]–[11]. In terms of the device intrinsic properties, it mainly refers to the layout structure of device and its surrounding topological environment.[14–17] Raine *et al.*[14–16] studied the effects of the ion mass and energy on the response of device and heavy ion-induced MBU sensitivity using ion track structure profile. The trajectory of incident ion penetrating through the target has also been studied, and some analytical algorithms were proposed for calculating the ion track structure in specific material.[18,19] Generally, the MBU characterization is becoming more crucial and highlighted in the field of SEEs.

In this work, we will first employ the simulation tool: multi-functional package for SEEs analysis (MUFPSA) simulation tool[20–22] to study the applicability of LET and explore its influence on MBU susceptibility. The MBU susceptibility of device induced by incident ions with the same LET will be further estimated and discussed. Given that the model of charge diffusion–collection and the radial distribution of ion track has been additionally developed in MUFPSA, the theoretical analysis about mapping the MBU multiplicity, MBU probability, and layout structure effects are studied and the radial track profiles are thereafter discussed.

*Project supported by the National Natural Science Foundation of China (Grant Nos. 11179003, 10975164, 10805062, and 11005134).
†Corresponding author. E-mail: j.liu@impcas.ac.cn
© 2013 Chinese Physical Society and IOP Publishing Ltd

2. Heavy ion irradiation

According to previous work,[14–17] it is reasonable to hypothesize that the over-layer and the active part of the testing electronic device are comprised of SiO_2 and Si, respectively. The specific dimensions of over-layer and active silicon film are extracted from Ref. [17]. The surface area of the hypothetical SRAM device for all the SVs is 1.15 μm^2, and it is assumed that the thickness values of over-layer and the silicon film of the SV are respectively 0.1 μm and 80 nm. To evaluate the MBU occurrence, 6×6 cells are defined as the sensitive volume (SV) and embedded into the active silicon film layer.

To represent real space radiation environment, heavy ion beams are selected as radiation source in our calculation, which are consistent with the heavy ion research facility in Lanzhou) (HIRFL) SEE testing experiments, including ions ^{40}Ar, ^{132}Xe, and ^{209}Bi. In Table 1 listed are the characteristic parameters of ion beams, including ion species, their associated energies, LET, and stopping ranges in silicon.

Table 1. Irradiated heavy ion effective LET and range in silicon, which are calculated by SRIM 2011.

Ions	Energy/MeV	Effective LET/ MeV·cm^2·mg^{-1}	Range/μm
^{40}Ar	3887.55	2.00	4860
	1534.60	4.00	1010
^{132}Xe	13538.79	16.00	2270
	4656.33	32.00	4444.18
	1097.52	62.00	80.45
^{209}Bi	6369.43	65.00	350.62
	4315.11	75.00	223.62

Generally, the SEU rates and cross section measurements can be appropriately described by Weibull fitting function as follows:

$$\sigma = \begin{cases} \sigma_{\text{sat}} \left\{ 1 - \exp\left[-\left(\dfrac{L - L_{\text{th}}}{W} \right)^{s} \right] \right\}, & L > L_{\text{th}}, \\ 0, & L < L_{\text{th}}, \end{cases} \quad (1)$$

where L_{th} is the onset LET threshold in MeV·cm^2·mg^{-1}, W is the Weibull width parameter also in MeV·cm^2·mg^{-1}, s is the dimensionless shape parameter, and σ_{sat} is the saturation cross section in cm^2.

The results of SEU cross section as a function of LET and Weibull function fitting are reported in Fig. 1. Accordingly, the data and curve demonstrate quite a decent agreement with each other. The SEU cross section sequentially approaches to the saturation as the LET increases. Specifically, we have $\sigma_{\text{sat}} = 3.1715 \times 10^{-10}$ cm^2, $L_{\text{th}} = 2$ MeV·cm^2·mg^{-1}, $W = 0.0193$ MeV·cm^2·mg^{-1}, $s = 0.1508$, from Weibull function fitting report. However, it is worth mentioning that a slight reduction is observed at the interval of ^{132}Xe and ^{209}Bi irradiation shown in the inset, and it is equally shown that more SEU cross sections are induced by lower LET of ^{132}Xe (62.00 MeV·cm^2·mg^{-1}) as compared with that by the higher LET of ^{209}Bi (65.00 MeV·cm^2·mg^{-1}). The interpretation of this result should factor ion species and energy (or LET) as has been presented at several different experimental facilities.[11] Thus, studies on the ion species and energy are necessary to further understand SEU susceptibility.

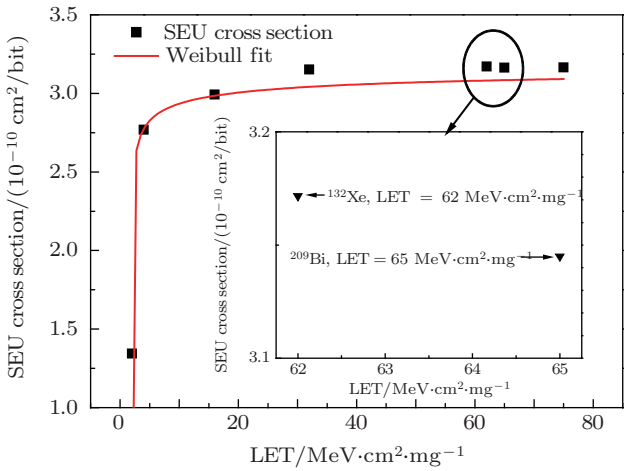


Fig. 1. (color online) SEU cross section versus LET for 90-nm simulated SRAM and Weibull distribution fitting. The inset displays the descending point.

As a representive of SEU susceptibility, the MBU sensitivities influenced by incident ion ^{132}Xe and ^{209}Bi with the same LET are studied. It is tacitly considered that SRIM 2011 calculated LET of different ions are acceptable as an accurate estimation. The results of LET with various energies for ^{132}Xe and ^{209}Bi are performed, giving the LET curves in Fig. 2.

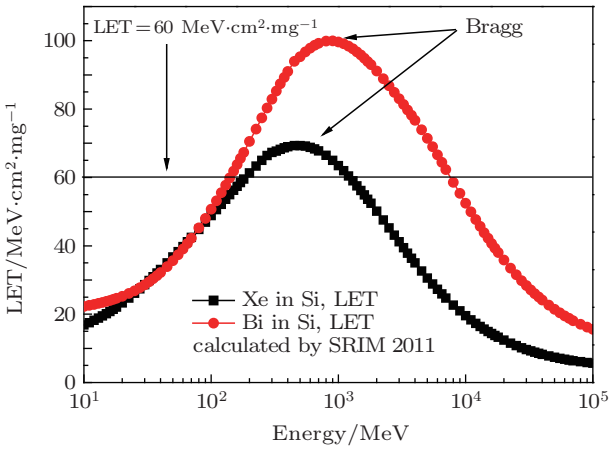


Fig. 2. (color online) Typical photographic results of LET as a function of ion energy for ion ^{132}Xe and ^{209}Bi.

According to the Bragg peak of LET emerging in Fig. 2, it is possible to obtain the same LET under the condition of the same ion species with different energies, even of different ion species. In the work, as the reduction in SEU cross section between ^{132}Xe and ^{209}Bi mentioned above, the case with the same LET value of about 60 MeV·cm^2·mg^{-1} is studied, corresponding to the horizontal line in Fig. 2. Table 2 gives the detailed values of energy and range in silicon of ^{132}Xe and ^{209}Bi.

Table 2. Parameters of ions ^{132}Xe and ^{209}Bi with about the same LETs but different energies.

Ions	Energy/MeV	Effective LET/MeV·cm^2·mg^{-1}	Range/μm
^{132}Xe	185.08	60.00	21.28
	1231.33		89.90
^{209}Bi	140.63	60.00	16.23
	7625.26		437.38

3. Results and discussion

The influence of LET on MBU susceptibility is investigated and discussed by MUFPSA with two goals that are to obtain the MBU multiplicity and probability and to investigate and identify the influence of radial distribution of ion tracks.

3.1. Obtaining the MBU multiplicity and probability

In MUFPSA, to reflect the actual physical process between incident ions and device, in the model for evaluating the MBU susceptibility the contributions of not only incident ions, but also reaction products surrounding the SVs are considered. Thus, the physical processes involved in MUFPSA include ionization, nuclear elastic and inelastic reactions, and multiple scattering. Additionally, all the SVs have been marked with numbers for visually mapping the MBU multiplicity. To quantify the MBU rates, the MBU probability is given as

$$\mathrm{MBU}_{\mathrm{probablity}} = \frac{\mathrm{MBU}}{\mathrm{SEU}} \times 100\%, \tag{2}$$

where SEU is the number of incident ions inducing at least one error or single event upset, and MBU is the number of incident ions inducing more than one error.

The Geant4-tool MUFPSA is then utilized to study the MBU multiplicity and probability, and its dependence on the incident angle and ions beam profile. During the simulation, the package of General Particle Source is invoked to run the 10^4 primary ions of various species and with different energies and incident angles. In addition, we have separately labeled every single cell with a specific number for distinctly detecting the MBU patterns.

Several common MBU patterns observed by MUFPSA are shown in Fig. 3. It is revealed that triple bit upset (TBU) has more shapes than double bit upset (DBU), while a strongly predominant TBU is identified — L-shaped. It is clear that the model of charge diffusion–collection in our simulator is indeed effective due to the capability of detecting the nonlinear bit errors. For instance, if a track traverses on the two SV surfaces, the sharing charge still has the capability of inducing a flipping on a third one. Thus, the feature of detecting nonlinear MBUs provides an accurate mapping of MBU probability and multiplicity. In the following, the detailed characteristics of the MBUs based on this feature are calculated and discussed.

The MBU sensitivities to heavy ions with the same LET but different energies are evaluated at isolated incident angles, plotted in Fig. 4. As expected, the MBU sensitivity increases with the increase of incident angle. The physical interpretation for that situation is the increases of the effective LET and the interactional probability between incident ions and the SVs. Additionally, no obvious differences are observed between the lower energy of ^{132}Xe and ^{209}Bi. It is, however, interesting to note that less MBU occurs in the case of the same ions with higher energy (especially the highest energy ^{209}Bi ions) than with lower energy. Therefore, it is elucidated that the incident ions with the same LET (or even the same ion species) can lead to different values of MBU probability.

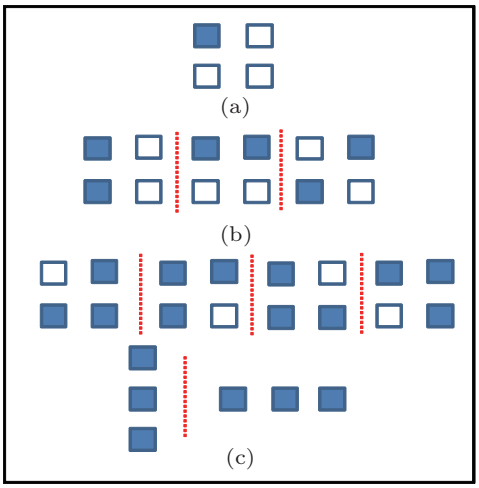


Fig. 3. (color online) Example of the MBU patterns with single bit upset (SBU), DBU, and TBU involved adjacent cells from observation of MUFPSA. Solid box denotes the flipped cell, open box represents the normal cell.

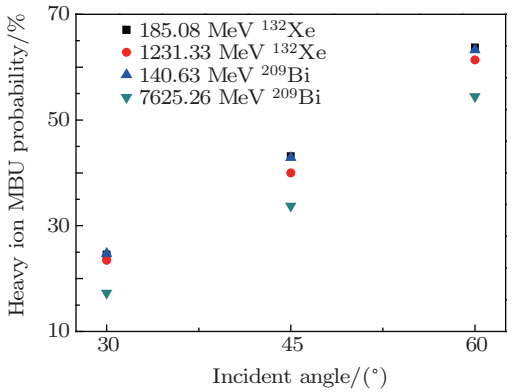


Fig. 4. (color online) Variations of the heavy ion MBU probability with the incident angle increasing from 30° to 60°.

As mentioned above, the influence of LET on multiple bit upset distribution should be taken into account. The percentages of single bit upset and multiple bit upset events versus incident angle for different simulated ions are reported in Fig. 5. The proportion of single bit upset and multiple bit upset

events directly displays the detailed information about multiple bit upset multiplicity and the corresponding percentage. Similarly, the results show that multiple bit upset probability is less in the case of the higher energy than in the case of lower energy. Taking the occurrence of triple-bit events for example, it is obviously shown that the observation probabilities of MBU (3) in Figs. 5(a) and 5(c) 12.08% and 11.64% are more than 10.62% and 7.06% in Figs. 5(b) and 5(d), respectively. However, it should be noted that incident ion ^{132}Xe 185.08 MeV/1231.33 MeV induces more multiple bit upset probabilities than ^{209}Bi 140.63 MeV/7625.26 MeV. Indeed, this characteristic directly verifies the above results in Fig. 4.

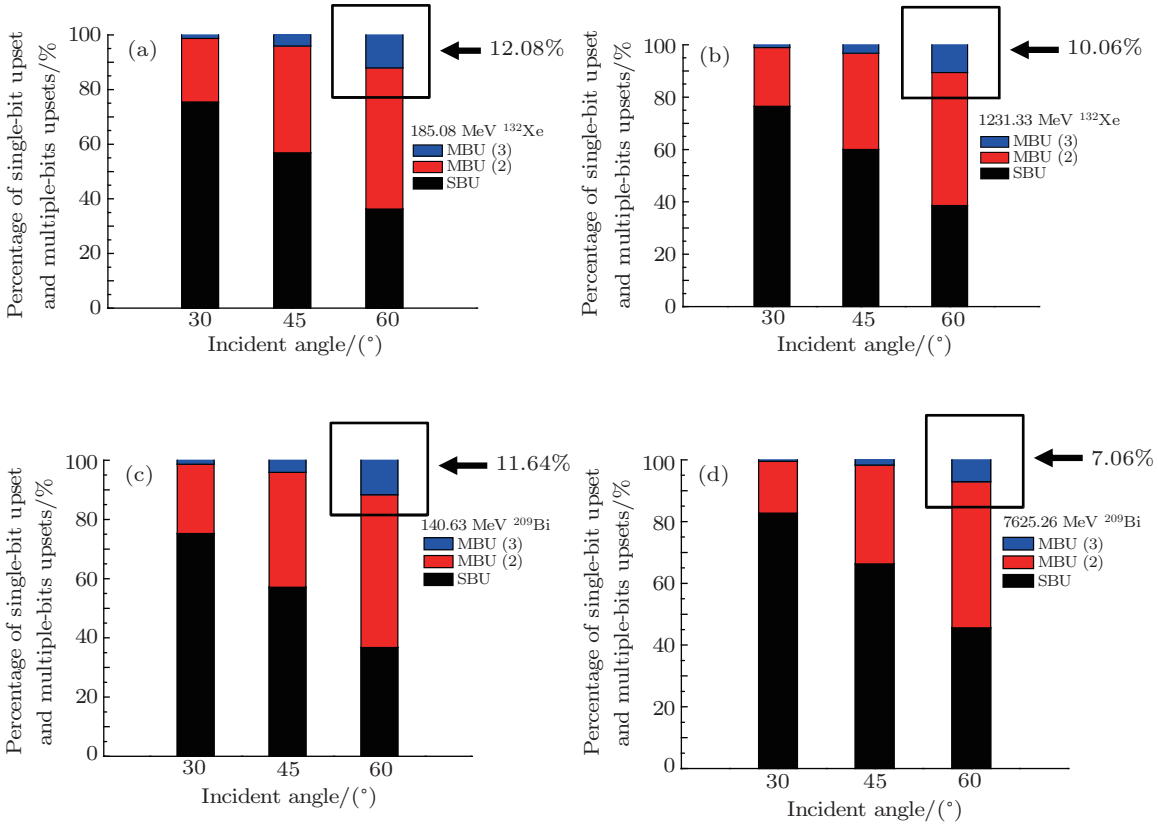


Fig. 5. (color online) Percentages of SBU and MBU versus incident angle for different ions but same LET: (a) ^{132}Xe 185.08 MeV, (b) ^{132}Xe 1231.33 MeV, (c) ^{209}Bi 140.63 MeV, and (d) ^{209}Bi 7625.26 MeV.

3.2. Investigating and identifying the influence of radial distribution of ion tracks

The MUFPSA tool is known to have the capability of quantifying the radial distribution of e^-/h^+ pairs and spatial charge deposition.[20–22] Besides, based on δ-ray theory, the maximum range of δ ray and the incident ion's relative velocity also play an indispensable role in analyzing MBU characteristics. Therefore, to identify and explain SBUs, i.e., MBUs, induced by different ion tracks, it is reasonable and effective to simulate the radial distribution of ion tracks with MUFPSA tool. To be specific, we make a detailed comparison between ^{132}Xe and ^{209}Bi in terms of radial ionization profile.

The relative parameters of incident ions that we evaluated for radial ionization profile are summarized in Table 3. It is indicated that the maximum radius of δ ray and relative velocity of the incident ions can change even more than one order of magnitude in the case of the same LET, which agrees well with the previously reported result.[23] Additionally, it is also revealed that the higher the ion energy, the higher the relative velocity is and the longer the range of δ rays is.

Table 3. Parameters of ions ^{132}Xe and ^{209}Bi with about the same LETs but different energies.

Ions	Energy/MeV	Maximum radius of δ rays/nm	Relative velocity
^{132}Xe	185.08	393	0.0548258
	1231.33	9310	0.1405198
^{209}Bi	140.63	115	0.0379906
	7625.26	92533	0.2719720

The radial distribution of e^-/h^+ pair density around the path of incident ions performed by MUFPSA is depicted in Fig. 6. From Table 3 and Fig. 6 it follows that MBU may emerge as long as the maximum range of ion tracks is long enough to reach and affect the neighboring SVs. Moreover,

according to the size of SV ($L = 179$ nm), the energy deposited is increasing with relative velocity decreasing. Therefore, incident ions ^{132}Xe and ^{209}Bi at the energies of 185.08 MeV and 140.63 MeV induce higher MBU probability than those at the energies of 1231.33 MeV and 7625.26 MeV.

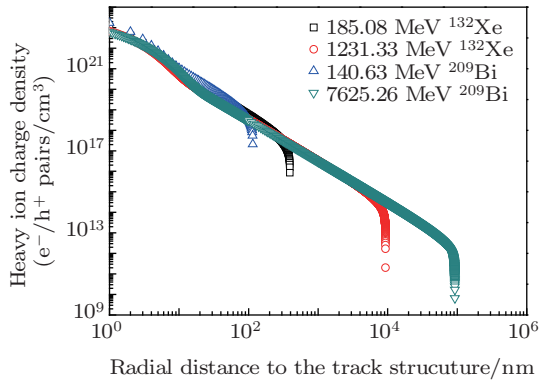


Fig. 6. (color online) MUFPSA simulation results of the radial pair density profile. All the ions are normally incident on the surface of the hypothetical device.

Based on the simple charge diffusion–collection mechanism, accumulated charge is calculated on condition that incident ions traverse in silicon within the depth of 80 nm as illustrated in Fig. 7. The dimension of the area is strictly defined by reference to the size of SV. As can be seen from Fig. 7, the accumulated charge is declining as the radius of area increases. In addition, most of the charges are accumulated in the innermost area of radius $0.5L$. However, it is interesting to note that ^{132}Xe 185.08 MeV has enough accumulated charge in the second innermost area to trigger MBUs, whereas the maximum range of δ-ray induced by ^{209}Bi 140.63 MeV cannot reach this part, although ^{209}Bi 140.63 MeV induced more charge in the first area. Thus, it explains why the incident ion ^{132}Xe 185.08 MeV can cause more MBU to occur than the ion ^{209}Bi 140.63 MeV as indicated in Fig. 5.

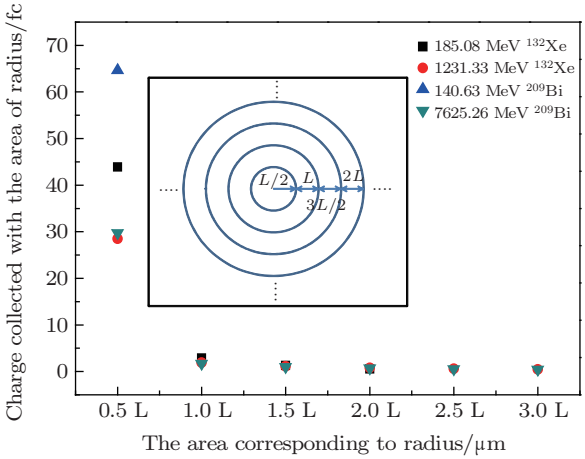


Fig. 7. (color online) Calculated charge collected within the area of radius versus the area corresponding to radius for different incident energies, with the inset showing the geometrical construction for this calculation.

4. Conclusions

In this paper an analytical Monte Carlo simulation tool — MUFPSA is proposed to model and analyze SEU characteristics, particularly the influence of LET on MBU susceptibility. According to the commonly-accelerated ion species in HIRFL SEE testing experimental facility, ions ^{40}Ar, ^{132}Xe, and ^{209}Bi are selected as incident ions for heavy ions irradiation on 90-nm hypothetical SRAM. One noticeable observation is the reduction of SEU cross section at the interchange point between ^{132}Xe and ^{209}Bi. Thus, the influence of ions with the same LET (60 MeV·cm^2·mg^{-1}) but different energy on MBU sensitivity is simulated and discussed.

MBU multiplicity and probability are investigated and quantified to study the validity and applicability of LET in SEUs. The results show that LET alone is not accurate enough to characterize SEUs because MBU distributions induced by incident ions with the same LET are different, particularly as an indication reflected in the MBU probability. Furthermore, two parameters derived from ion track structure, i.e., track radius and ion relative velocity, are taken into consideration, which turns out that the ability for incident ions to trigger MBUs follows the following sequence: ^{132}Xe 185.08 MeV> ^{209}Bi 140.63 MeV> ^{132}Xe 1231.33 MeV> ^{209}Bi 7625.26 MeV. The interpretation is that slower ion-velocity would produce higher radial density of e$^-$/h$^+$ pairs, and hence causing more charge to be deposited. Consequently, we conclude that the applicability of LET in SEUs still needs more investigation.

References

[1] Connel L W, McDaniel P J, Prinja A K and Sexton F W 1995 *IEEE Trans. Nucl. Sci.* **42** 73

[2] Inguimbert C and Duzellier S 2004 *IEEE Trans. Nucl. Sci.* **51** 2805

[3] Schwank J R, Shaneyfelt M R, McMorrow D, Ferlet-Cavrois V, Dodd P E, Heidel D F, Marshall P W, Pellish J A, LaBel K A, Rodbell K P, Hakey M, Flores R S, Swanson S E and Dalton S M 2010 *IEEE Trans. Nucl. Sci.* **57** 1827

[4] Giot D, Roche P, Gasiot G and Harboe-Sorensen R 2007 *IEEE Trans. Nucl. Sci.* **54** 904

[5] Warren K M, Sierawski B D, Reed R A, Weller R A, Carmichael C, Lesea A, Mendenhall M H, Dodd P E, Schrimpf R D, Massengill L W, Tan Hoang, Hsing Wan, De Jong J L, Padovani R and Fabula J J 2007 *IEEE Trans. Nucl. Sci.* **54** 2419

[6] Zhang K Y, Guo H X, Luo Y H, Fan R Y, Chen W, Lin D S, Guo G and Yan Y H 2011 *Chin. Phys. B* **20** 068501

[7] Stapor W J, McDonald P T, Knudson A R and Campbell A B 1988 *IEEE Trans. Nucl. Sci.* **35** 1585

[8] Dodd P E, Schwank J R, Shaneyfelt M R, Ferlert-Cavrois V, Paillet P, Baggio J, Hash G L, Felix J A, Hirose K and Saito H 2007 *IEEE Trans. Nucl. Sci.* **54** 889

[9] Dodd P E, Schwank J R, Shaneyfelt M R, Felix J A, Paillet P, Ferlert-Cavrois V, Baggio J, Reed R A, Warren K M, Weller R A, Schrimpf R D, Hash G L, Dalton S M, Hirose K and Saito H 2007 *IEEE Trans. Nucl. Sci.* **54** 2303

[10] Warren K M, Weller R A, Mendenhall M H, Reed R A, Ball D R, Howe C L, Olson B D, Alles M L, Massengill L W, Schrimpf R D, Haddad N F, Doyle S E, McMorrow D, Melinger J S and Lotshaw W T 2005 *IEEE Trans. Nucl. Sci.* **52** 2125

[11] Reed R A, Weller R A, Mendenhall M H, Lauenstein J M, Warren K M, Pellish J A, Schrimpf R D, Sierawski B D, Massengill L W, Dodd P E, Schaneyfelt M R, Felix J A, Schwank J R, Haddad N F, Lawrence R K, Bowman J H and Conde R 2007 *IEEE Trans. Nucl. Sci.* **54** 2312

[12] Zhang K Y, Guo H X, Luo Y H, He B P, Yao Z B, Zhang F Q and Wang Y M 2009 *Acta Phys. Sin.* **58** 8651 (in Chinese)

[13] Zhang Q X, Hou M D, Liu J, Jin Y F, Zhu Z Y and Sun Y M 2004 *Acta Phys. Sin.* **53** 566 (in Chinese)

[14] Raine M, Hubert G, Gaillardin M, Artola L, Paillet P, Girard S, Sauvestre J E and Bournel A 2011 *IEEE Trans. Nucl. Sci.* **58** 840

[15] Raine M, Hubert G, Gaillardin M, Paillet P and Bournel A 2011 *IEEE Trans. Nucl. Sci.* **58** 2607

[16] Raine M, Gaillardin M, Sauvestre J, Flament O, Bournel A and Aubry-Fortuna V 2010 *IEEE Trans. Nucl. Sci.* **57** 1892

[17] Giot D, Roche P, Gasiot G, Autran J L and Sorensen R H 2007 *9th Eur. Conf. Radiation and Its Effects on Components and Systems (RADECS),* Septemper 10–14, Deauville, France, p. 1

[18] Cucinotta F A, Katz R, Wilson J W and Dubey R R 1996 *Faculty Publications*, p. 62

[19] Waligorski M P R, Hamm R N and Katz R 1986 *Radia. Meas.* **11** 309

[20] Geng C, Liu J, Xi K, Zhang Z G, Gu S, Hou M D, Sun Y M, Duan J L, Yao H J and Mo D 2013 *Chin. Phys. B* **22** 059501

[21] Geng C, Liu J, Zhang Z G, Hou M D, Sun Y M, Xi K, Gu S, Duan J L, Yao H J, Mo D and Luo J 2013 *Sci. China Ser. G: Phys. Mech. Astron.* in press **56** Doi:10.1007/s11433-013-5101-x

[22] Geng C, Liu J, Zhang Z G, Xi K, Gu S, Hou M D, Sun Y M, Duan J L, Yao H J, Mo D and Luo J 2013 *Chin. Phys. C* **37** 066001

[23] Meftah A, Brisard F, Costatini J M, Hage-Ali M, Stoquert J P, Studer F and Toulemonde M 1993 *Phys. Rev. B* **48** 920